Chemical Engineering Journal 162 (2010) 301–306

Contents lists available at ScienceDirect

Chemical Engineering Journal

journal homepage: www.elsevier.com/locate/cej

Effect of diffusion on enzyme activity in a microreactor

Jan W. Swarts, Ruben C. Kolfschoten, Mieke C.A.A. Jansen, Anja E.M. Janssen*, Remko M. Boom

Wageningen University, Food Process Engineering, Bomenweg 2, 6703 HD Wageningen, The Netherlands

ARTICLE INFO

Article history:
Received 17 October 2009
Received in revised form 18 April 2010
Accepted 22 April 2010

Keywords:
Microreactors
β-Galactosidase
Diffusion limitation
Computational fluid dynamics

ABSTRACT

To establish general rules for setting up an enzyme microreactor system, we studied the effect of diffusion on enzyme activity in a microreactor. As a model system we used the hydrolysis of *ortho*-nitrophenyl-β-D-galactopyranoside by β-galactosidase from *Kluyveromyces lactis*. We found that the Michaelis–Menten kinetic parameters were similar at the microscale and bench scale. With residence times below a few seconds, diffusion effects limited the reaction rate and therefore reduced the conversion per volume of enzyme microreactor. The critical residence time where diffusion limits the conversion increased quadratically with channel width, increased with enzyme concentration, and decreased with substrate concentration. These general rules can be used for choosing parameters when setting up an enzyme microreactor system. To use an enzyme microreactor efficiently, diffusion effects should be taken into account.

1. Introduction

Over the years microreactors have been credited with many advantages over conventional systems. Due to their small internal dimensions, the diffusion of heat and mass can be very rapid. Furthermore, their limited use of chemicals and energy can reduce cost and lessen environmental impact.

Enzymes have been used in microfluidic systems to catalyze the production of very specific molecules. In the 1990s, enzyme microreactors were first used for enzyme assays [1,2]. Enzyme microfluidic systems were also used to determine enzyme kinetics [3–6], screen enzymes in droplets [7,8], and to investigate temperature effects on enzyme activity [9,10] and study cascaded enzymatic reactions [3,11,12].

The reaction rate of an enzyme is determined by its activity and the availability of the substrate at the enzyme's active site. In a system where the substrate has to bridge a large distance to the active site, the effective reaction rate could be limited. Due to the small dimensions, typically 10–100 μm, microreactors could reduce these diffusional limitations of enzymes.

The effect of diffusion on enzyme activity was studied as early as in the 1960s by Lilly and co-workers [13–15]. That work focused on the effect of diffusion on the enzyme activity of β-galactosidase and ficin immobilized on membranes. The effect of diffusion on enzyme activity in microreactors was discussed in some papers. The diffusion limitation on the effective enzyme activity was hinted by Kanno et al. [16], but was not investigated. Maruyama et al. [17] did investigate the effect of diffusion, but they used an excess of enzyme to make diffusion dominant. More recently, Ristenpart et al. [4] investigated enzyme kinetics in a microsystem with both diffusion and reaction limitation. Their article focused on the rapid extraction of kinetic data from experimental results, rather than on estimating the effect of the limitation.

In our research we investigated the effect of diffusion limitation on the β-galactosidase catalyzed cleavage rate of *ortho*-nitrophenyl-β-D-galactopyranoside (*o*-NPG) in a microreactor. We chose this reaction as a model system; it results in *ortho*-nitrophenol (*o*-NP), a yellow substance, and galactose, which is colorless. First, the kinetics of this reaction were determined at the bench scale and microscale and were compared. Second, the reaction was tested under diffusion limiting circumstances in a microreactor. Finally, the effect of diffusion combined with a reaction was studied using computer models and theoretical parameters. The results from this research show the conditions under which the short diffusion paths in microreactors eliminate diffusion limitation in an enzymatic reaction.

2. Theory

In the enzyme microreactor discussed in this paper, a Y-shaped junction brings a substrate and an enzyme solution into a single laminar flow reaction channel. Fig. 1 depicts this reaction channel schematically. A flow with enzyme and a flow with substrate enter the left side of the rectangle. Even though the two laminar streams in the microchannel do not mix by convection, there is molecular diffusion between them. Substrate and enzyme start to diffuse over the boundary between the two aqueous flows. The substrate is a smaller molecule, so it diffuses more quickly into the

* Corresponding author. Tel.: +31 317 48 22 31; fax: +31 317 48 22 37.
E-mail address: Anja.Janssen@wur.nl (A.E.M. Janssen).

1385-8947/$ – see front matter © 2010 Elsevier B.V. All rights reserved.
doi:10.1016/j.cej.2010.04.040

Nomenclature

D	diffusion coefficient ($m^2\ s^{-1}$)
Da_{II}	second Damköhler number
[E]	enzyme concentration ($g\ L^{-1}$)
K_m	Michaelis–Menten constant (mM)
L_D	distance at which diffusion is theoretically complete (m)
[P]	product concentration (mM)
$[P]_t$	product concentration at time t (mM)
$[S]_0$	initial substrate concentration (mM)
t	time (s)
t_D	typical diffusion time (s)
t_r	typical reaction time (s)
v_0	initial enzyme reaction rate ($\mu mol\ s^{-1}\ g\ enzyme^{-1}$)
V_{max}	maximum enzyme reaction rate ($\mu mol\ s^{-1}\ g\ enzyme^{-1}$)
x	distance in flow direction (m)
y	diffusion distance (m)

enzyme stream. The enzyme diffuses much more slowly into the substrate stream. The curved lines indicate the theoretical fronts of the diffusing molecules.

The reaction takes place at locations where both substrate and enzyme are present, indicated by the dark gray area in Fig. 1. From position L_D onwards in the x-direction, the substrate has distributed more or less evenly over both streams and the enzyme reaction should be at its kinetically determined rate over the whole width of the channel. The position of L_D relative to the total reaction channel length is an indication of the importance of diffusion limitation, resulting in a significantly lower product concentration at the exit of the channel. In the extreme case that diffusion is very fast compared to the other processes (i.e. the reaction mixture is ideally mixed at $t = 0$ s); the analytical solution, shown in Eq. (1), should apply:

$$K_m \ln\left(\frac{[S]_0}{[S]_0 - [P]_t}\right) + [P]_t = V_{max}[E]\,t \quad (1)$$

In this equation, K_m is the Michaelis–Menten constant (mM), $[S]_0$ is the initial substrate concentration (mM), $[P]_t$ is the product concentration at residence time t (mM), V_{max} is the maximum enzyme reaction rate ($\mu mol\ s^{-1}\ g\ enzyme^{-1}$), [E] is the enzyme concentration ($g\ enzyme\ m^{-3}$), and t is the residence time (s).

The second Damköhler number (Da_{II}), a dimensionless number, is often used to express the ratio of diffusion time to reaction time. Although the use of this number has been proposed for enzyme microreactor systems [18], it is not used extensively:

$$Da_{II} = \frac{t_D}{t_r} = \frac{y^2}{D} \cdot \frac{v_0[E]}{[S]_0} \quad (2)$$

$$t_D = \frac{y^2}{D} \quad (3a)$$

$$t_r = \frac{[S]_0}{v_0[E]} \quad (3b)$$

In Eq. (2), t_D is the characteristic time needed for diffusion (s), t_r is the characteristic reaction time (s), y is the diffusion distance (m), v_0 is the initial reaction rate ($\mu mol\ s^{-1}\ g\ enzyme^{-1}$), and D is the diffusion coefficient ($m^2\ s^{-1}$). Eq. (2) is composed of the parts of Eqs. (3a) and (3b). Eq. (2) assumes that the reaction will continue at a zero-order initial rate. By inserting the Michaelis–Menten kinetic equation in the Damköhler number we obtain:

$$Da_{II} = \frac{t_D}{t_r} = \frac{y^2}{D} \cdot \frac{V_{max}[S][E]}{(K_m + [S])[S]} = \frac{y^2}{D} \cdot \frac{V_{max}[E]}{(K_m + [S])} \quad (4)$$

Eq. (4) is again composed of the characteristic diffusion and reaction times:

$$t_D = \frac{y^2}{D} \quad (5a)$$

$$t_r = \frac{(K_m + [S])}{V_{max}[E]} \quad (5b)$$

The calculations of the characteristic diffusion times (Eq. (5a)) and reaction times (Eq. (5b)) indicate how parameters influence the ratio between the two. For instance, a high enzyme concentration leads to a low characteristic reaction time and consequently to less kinetic limitation.

Over the course of a reaction, conversion progresses, and the substrate concentration decreases. As a result, the value of Da_{II} calculated using Eq. (4) is not constant as opposed to the value calculated using Eq. (2). With very low substrate concentrations, the reaction rate approaches zero. A full conversion, as assumed in the Da_{II} number, will only be reached after an infinitely long time.

To avoid complications due to the 100% conversion assumption, we propose a critical time as an alternative to the Da_{II} number. We calculated the ratio of the product concentration exiting the microreactor including diffusion (from numerical models) to the concentration without diffusion limitation (from Eq. (1)) at various residence times. For the critical time, we chose the residence time at which this ratio is 0.9. This critical time is an indicator of the effect of diffusion on reactor efficiency.

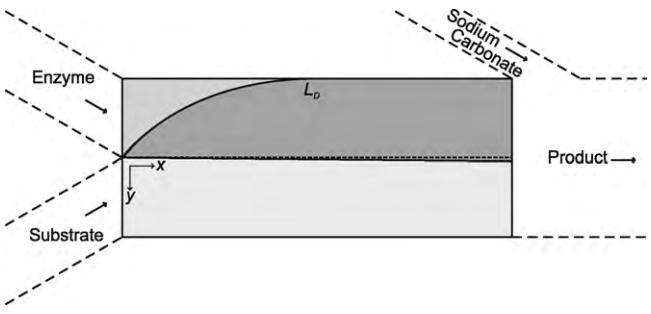

Fig. 1. Schematic diffusion profiles of substrate (bottom to top) and enzyme (top to bottom) in the microreactor. The dotted line indicates the original position of the interface; L_D indicates the position in x-direction where diffusion of substrate is complete. Dashed lined indicate the supplying and exiting channels not taken into consideration for calculations.

3. Materials and methods

3.1. Chemicals

The β-galactosidase from *K. lactis* (in solution, ≥3000 U/mL), *ortho*-nitrophenol (*o*-NP, 98%), potassium phosphate (99%), and sodium carbonate (99%) were purchased from Sigma–Aldrich (Milwaukee, WI). The *ortho*-nitrophenyl-β-D-galactopyranoside (*o*-NPG) was obtained from Fluka (Steinheim, Germany). The cobalt (II) chloride (hexahydrate) was purchased from ICN Biomedicals Inc. (Aurora, OH). Milli-Q water (Millipore, Billerica, MA) was used for the experiments discussed in this study.

3.2. Experiments on bench scale

At 23 °C, two 150 mL buffer solutions were mixed in a 500-mL stirred vessel with baffles and a 3-blade propeller type stirrer at 350 rpm. Both buffers contained 25 mM of sodium phosphate,

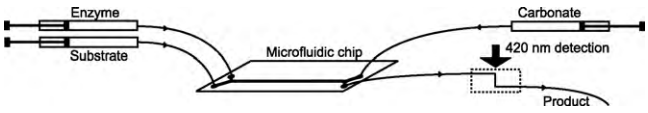

Fig. 2. Schematic representation of the experimental setup; enzyme and substrate are combined on-chip, at the end of the reaction channel, sodium carbonate is added to stop the reaction. All fluids exit the channel and pass through a *z*-shaped cell for detection at 420 nm.

15 μM cobalt chloride, and were set to pH 7.3 using sodium hydroxide. One buffer contained β-galactosidase at a concentration of 0.2 g L^{-1}. The other buffer contained *o*-NPG at concentrations varying from 1 to 20 mM. During the first 2 to 4 min, 0.5 mL samples were taken and mixed with 0.5 mL 1% (w/w) sodium carbonate. Addition of sodium carbonate resulted in a hundredfold lower activity (results not shown), which ensured no significant reaction after sampling. The concentration of *o*-NP was measured with a spectrophotometer at 420 nm. The linear part of the *o*-NP concentration vs. time plots (9–11 samples, $R^2 > 0.995$) was used to calculate the initial enzyme activity.

3.3. Experiments on microscale

The microscale enzymatic reaction was carried out at room temperature (20–22 °C). The two aqueous streams were combined on-chip. The microchannels were on average 83 μm wide and 40 μm deep and were isotropically etched in a microchip by Micronit (Enschede, the Netherlands). A schematic view of the chip is shown in Fig. 2. The total microchannel volume on-chip was 0.113 μL. An in-house constructed PEEK chipholder facilitated the connections between the chip and capillaries which supplied the fluids. These fused silica capillaries from Bester (Amstelveen, the Netherlands) have a 50-μm diameter and were connected to SGE 1 mL luer lock syringes (Austin, TX). The syringes were placed in Harvard Apparatus Pico Plus 11 syringe pumps (Holliston, MA).

The enzyme solution (approximately 0.2 g L^{-1}) and the substrate solution (*o*-NPG concentration varying from 1 to 20 mM) were prepared with a 25 mM potassium phosphate buffer with 15 μM Co^{2+} set to pH 7.3. The two solutions were placed on the same syringe pump and consequently pumped at the same rate. The solutions (shown at the left in Fig. 2) were combined at a 1:1 volumetric ratio. Just before exiting the chip, this stream was joined by a 1% (w/w) sodium carbonate in Milli-Q stream (top-right in Fig. 2). The combined enzyme and substrate flow was matched with this carbonate solution in a 1:1 volumetric ratio. Due to the inhibiting effect of sodium carbonate (even at fairly low concentrations) and the relatively fast diffusion (shorter diffusion distance due the compressing of streams and the small molecule), reaction stoppage was assumed to be instantaneous. The enzyme diffuses into the substrate domain much more slowly than the substrate into the enzyme domain, and in almost every case an enzyme molecule would move from an area with both enzyme and substrate to another area with both enzyme and substrate. Therefore, the net effect on activity was negligible.

In most cases, the Reynolds number of the fluid was below unity. Depending on the flow rates and position in the system, it varied from approximately 0.02–25. With these values, laminar flow could be assumed. Therefore, the dominant type of mixing was by means of molecular diffusion. In practice, there are some limitations to using very high flow rates. For instance, the pressure in the system could become very high. This could result in leakage at connections. Furthermore, depending on the size of the channels and the viscosity of the more gas-like fluids, the Reynolds number could become too high to assume laminar flow and simple mixing by diffusion. However, this latter case is very unlikely for fluids.

The reaction mixture exited the chip through a fused silica capillary, which was connected to a LC Packings U–Z View capillary flow cell (Sunnydale, CA). The total post-chip volume until detection was 0.8–1.2 μL. This flow cell was placed in an UltiMate UV–VIS detector from Dionex (Sunnydale, CA) and had a 10-mm light path for accurate measurements. The measured absorbance at 420 nm was correlated to the *o*-NP concentration. The *o*-NP concentration was plotted against the residence time (inversely proportional to the flow rate), and from the linear part of this graph the initial activity was calculated.

Two methods were used to investigate the effect of diffusion limitation on enzyme reactions in practice. In the first method, the original 83 μm wide microchannel was used, but both the enzyme concentration and the flow rates were increased by a factor of 10. The second method was to increase the time needed for diffusion by using a wider microchannel. The same fluids as with the kinetic experiments were pumped through microchannels with effective channel widths of 183 and 283 μm.

3.4. Computer models

Two-dimensional numerical models were constructed to calculate the concentration of all components at any position in the channel. The models were constructed with COMSOL Multiphysics from COMSOL (Burlington, MA). Similar to Fig. 1, two rectangular shapes sharing one long side were used to represent the domains of the two aqueous streams. As both streams are laminar and have the same flow rate, we could assume that the fluids would stay in their initial domains. All other components (*o*-NPG, *o*-NP, galactose, and β-galactosidase) were free to diffuse over the interface between the two domains.

The two rectangular fluid domains were 41.5 μm wide (equal to real effective diffusion distance) and 2 mm long. The real length of the channel was 34 mm. Assuming constant volumetric flow rate, the superficial fluid velocity was scaled proportionally to the ratio between the real length and the model length. The diffusion coefficients D of all diffusing components in water were calculated using the Wilke–Chang equation [19]. These coefficients were 0.64×10^{-9} m^2 s^{-1} for *o*-NPG, 0.94×10^{-9} m^2 s^{-1} for *o*-NP, 0.85×10^{-9} m^2 s^{-1} for galactose, and 0.047×10^{-9} m^2 s^{-1} for β-galactosidase.

The reaction was modeled using Michaelis–Menten kinetics and parameters from microscale experimental results. Combinations of substrate concentration and initial activity were fitted to Michaelis–Menten kinetics using Athena Visual Studio V12.0 (Athena Visual Studio, Naperville, IL).

4. Results and discussion

4.1. Enzyme kinetics

Kinetic experiments were conducted at room temperature at both bench scale and microscale. Microscale experiments were conducted at slightly lower temperatures than at bench scale (by approximately 2 °C). As the results will show, this did not affect the enzyme activity very much. Fig. 3 shows the initial activities from experiments and the fitted model on microscale (Fig. 3a) and bench scale (Fig. 3b). The activity is expressed as the number of micromoles produced per second per gram of the original enzyme solution. The kinetic parameters obtained from these fitted models are summarized in Table 1.

Fig. 3 shows that for increasing substrate concentrations, the enzyme activity increases. The initial steep slope of the activity vs. substrate curve and the subsequent leveling off is consistent with Michealis–Menten kinetics. The values for K_m are somewhat lower, but in the same range as those from the literature; Cavaille and Combes [20] and Dickson et al. [21] both reported a K_m of

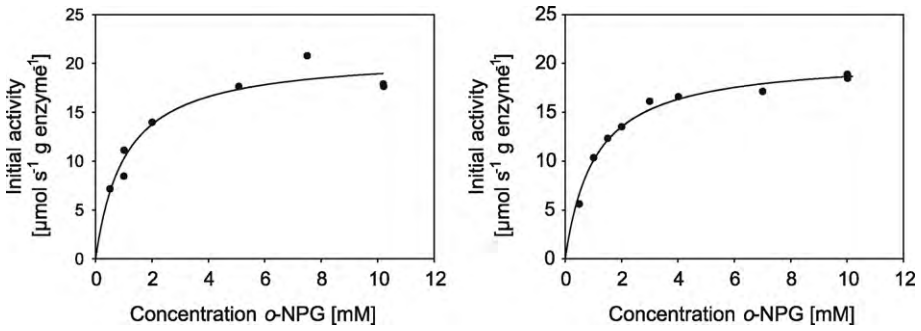

Fig. 3. Initial β-galactosidase activity as function of the *o*-NPG concentration on (a) microscale and (b) bench scale, symbols indicate experimental findings, drawn lines indicate model based on fitted kinetic parameters.

Table 1
Kinetic parameters and 95% confidence interval determined from microscale and bench scale experimental results.

Parameter	Microscale	Bench scale
V_{max}	20.9 ± 2.3 μmol s^{-1} g enzyme^{-1}	20.6 ± 1.0 μmol s^{-1} g enzyme^{-1}
K_m	1.04 ± 0.45 mM	1.05 ± 0.21 mM

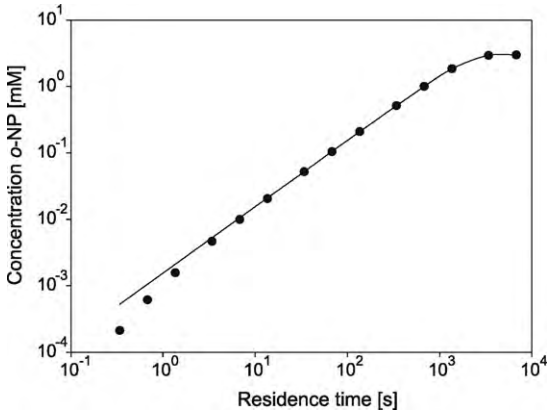

Fig. 4. Concentration of *o*-NP from the numerical COMSOL model (symbols) and the analytical equation (line) at different residence times.

about 1.7 mM. The values for the kinetic parameters as presented in Table 1 are very close for both experimental scales.

Fig. 4 shows the product concentration in the microchannel with increasing residence times. The results from the numerical COMSOL model were compared to the analytical solution of Eq. (1). Fig. 4 shows that the numerical results generally correspond to the analytical solution. With increasing residence times, the product concentration increases. Eventually, the *o*-NP concentration levels off at 3 mM, which corresponds to 100% conversion. Only at residence times below 10 s, the two models give different results, due to diffusion limitation. The results from experiments to determine the kinetic parameters in Fig. 3a, were typically obtained at residence times of around 30 s. Fig. 4 shows that ignoring the effect of diffusion limitation at these concentrations yields a 2% overestimation of the conversion. At these residence times, this overestimation is negligible, but it becomes significant at higher flow rates (i.e. smaller residence times).

4.2. Diffusion limitation in enzyme microreactors

Two methods were employed to investigate the effect of diffusion on product concentration: the use of wider microchannels and the combination of a high enzyme concentration with high flow rates. Fig. 5 shows the effect of microchannels of 183 μm (Fig. 5a) and 283 μm (Fig. 5b). Fig. 5a and b shows the increasing product concentration with increasing residence times, as obtained from the analytical solution (Eq. (1)), the numerical model, and experiments. The analytical solution yields much higher product concentrations than either the experiments or the numerical solution, indicating diffusion limitation in the latter two cases. The numerical and experimental results are in agreement, indicating that the lower concentrations are indeed caused by diffusion limitation. The models can therefore be used to investigate the effect of diffusion.

As shown in Fig. 5a and b, diffusion limitation clearly increased with wider channels, which was expected. The maximum diffusion distance in this microchannel is half the channel width. By increasing the channel width from 83 to 183 and 283 μm, the characteristic diffusion time increased by a factor of 4.9 and 11.6 (quadratically, according to Eq. (3a)), while the total reaction volume increased linearly by factors of 2.2 and 3.4, respectively.

Similar results were obtained by using the original 83 μm wide channels with a tenfold higher flow rate and enzyme concentration.

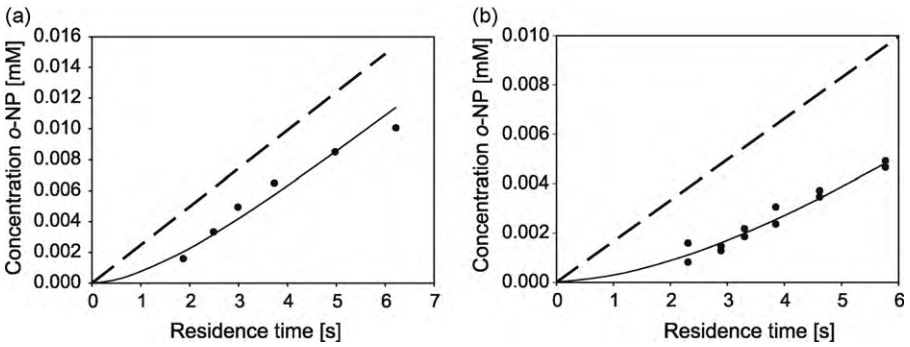

Fig. 5. The *o*-NP (product) concentration as function of the residence time; the dashed line represents the analytical solution, the solid line the numerical solution, and the symbols are the experimental results. The widths of the microchannels are: (a) 183 μm and (b) 283 μm.

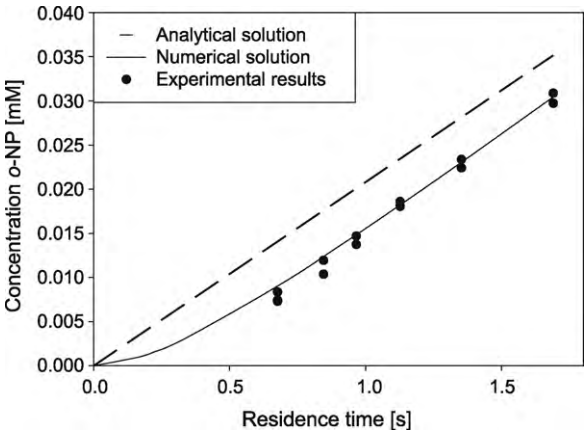

Fig. 6. The *o*-NP (product) concentration as function of residence time; dashed line for analytical solution, solid line for numerical solution, and symbols for experimental results. Microchannel with a width of 83 μm. The enzyme concentration is 10 times higher than in the experiments shown in Figs. 4 and 5.

This means that in the right-hand term of Eq. (1), V_{max} is constant, [E] is 10 times higher, and t is 10 times lower. In absence of diffusion limitation, the product concentration should be the same. However, Fig. 6 shows that diffusion limitation is important at all residence times (albeit relatively more important at lower residence times). This effect was predicted by the numerical model, which shows that diffusion limitation is indeed the cause of the reduction in product concentration.

The numerical models corresponded well with experimental results, as was shown in Figs. 5 and 6. We could therefore use these models to study the effect of the system parameters on the critical time, where diffusion caused a 10% reduction in product concentration. The enzyme reaction was kept the same, but parameters such as channel width and enzyme and substrate concentrations were varied to investigate the contribution of diffusion under these circumstances. Fig. 7 shows the results of variation of the model parameters.

Fig. 7a shows the efficiency of the system (the ratio is from numerical and analytical calculations; it is a indicator of diffusion limitation). As a residence time approaches 0 s, the substrate and enzyme are completely separated, and the efficiency is 0. At longer times, a uniform distribution of all components is obtained, and the actual reaction rate becomes equal to the intrinsic reaction rate. The efficiency therefore approaches 1.

Fig. 7a shows that with increasing channel widths it takes longer to approach the analytical result. To illustrate this, Fig. 7b shows the critical time, when the numerical result is 90% of the analytical result. This is shown as a gray dotted line in Fig. 7a. Here, diffusion effects caused a 10% limitation on the effective reaction rate. This critical time was plotted against the maximum diffusion distance in the microchannel, which is the distance the substrate has to travel to the enzyme (equal to half the channel width).

The effect of a wide range of enzyme concentrations on the critical time is shown in Fig. 7c. The critical time is fairly constant at 3.5–4 s up to an enzyme concentration of 1 g L^{-1}. At higher enzyme concentrations the critical time slightly increases to about 6 s. At low enzyme concentrations (<1 g L^{-1}) diffusion is apparently fast enough to supply the enzyme with substrate. At higher enzyme concentrations, the reaction is faster, leading to local depletion of substrate. At very high enzyme concentrations (100 g L^{-1} and higher) any substrate would be converted very quickly. The analytical solution gives a 99% conversion in slightly more than 2 s. Consequently, the critical time would no longer be an expression of diffusion limitation.

Fig. 7d shows the effect of substrate concentration on the critical time. At low substrate concentrations the critical time was high; with increasing concentrations the critical time decreased. When we only looked at diffusion of the substrate, different substrate concentrations did not change the shape of the theoretical diffusion front (curved line in Fig. 1). At the diffusion front, the concentration started to become non-zero, reaching the bulk concentration

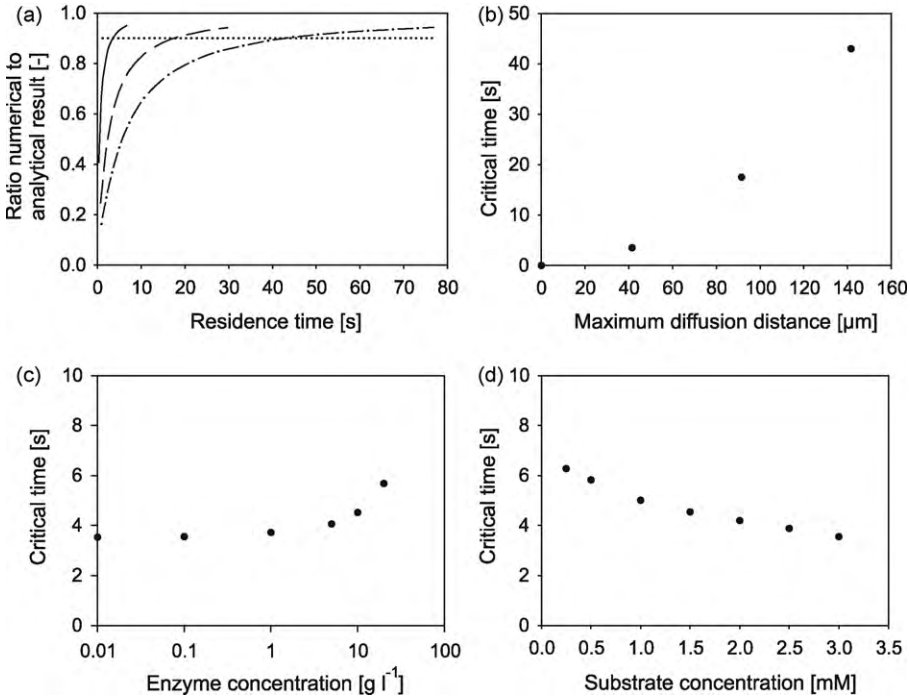

Fig. 7. Standard reaction conditions of 83 μm wide channel, 1 g L(1 enzyme, and 1 mM substrate were varied, one parameter each time. (a) Effect of different channel widths; the ratio of product concentration from numerical models to analytical solution is plotted against the residence time for different channel widths (solid line is 83 μm, dashed line is 183 μm, dash-dot-dashed line is 283 μm), (b) effect of different channel widths; critical time at which this ratio is 0.9 vs. maximum diffusion distance (equal to half the channel width), (c) critical time vs. enzyme concentration on a logarithmic scale, and (d) critical time vs. substrate concentration.

towards the original substrate channel. This concentration profile is similar to an error function. When we included reaction, the shape of the front changed, depending on this reaction.

Comparing the results of Fig. 7b–d with the Da_{II} number from Eq. (2), and its corresponding characteristic diffusion and reaction time from Eqs. (5a) and (5b), we can see similarities and differences. Fig. 7b shows that with increasing diffusion distances, the critical time increases quadratically, as does the Da_{II} number due to the increased diffusion time (Eq. (5a)). The Da_{II} number thus also predicts more diffusion limitation with an increased channel width.

According to Eq. (5b), the enzyme concentration should correspond inversely to the extent of diffusion limitation. However, numerical studies (Fig. 7c) showed an increase of the critical time, i.e. an increase in diffusion limitation, after a nearly constant level at the beginning. Initially, the enzyme concentration and the total reaction rate were so low that the critical time was purely diffusion driven. With increasing enzyme concentrations, substrate was depleted around the enzyme and caused a lower reaction rate per gram of enzyme due to Michaelis–Menten kinetics.

Again, according to Eq. (4), the Da_{II} should scale inversely with the term (K_m + [S]). A low [S] in Eq. (5b) will result in a lower limit for the characteristic reaction time. When [S] is significant relative to K_m, the characteristic reaction time will be higher. Thus, diffusion limitation at higher substrate concentrations is less likely. Similarly, the critical time from numerical studies (Fig. 7d) decreased with increasing substrate concentrations.

As the Da_{II} number assumed zero-order kinetics and one-dimensional Fickian diffusion, we expected deviations, with more complex cases. The enzyme we used followed Michealis–Menten kinetics and diffusion results in a concentration gradient rather than a propagating substrate front with a uniform substrate concentration behind it. The effect of varying parameters on the Da_{II} number corresponded with our numerical findings regarding the channel width and the substrate concentration, but differed regarding the enzyme concentration. The numerical model was a valuable tool added to the use of dimensionless numbers, as it can deal with non-ideal systems, demonstrated by the variation of the enzyme concentration.

Even though this study focused on Michaelis–Menten kinetics, and some of the relations are only valid for this type of kinetics, we suggest that the approach can be adapted to other kinetics such as ternary-complex or Ping-Pong mechanisms. *The approach for both the mathematical derivation and experimental work will be similar to the work described in this article.*

We studied a microreactor under laminar (creep) flow conditions, which implies that mixing by convection does not take place. Many mixing methods have been proposed in microfluidic technology which would enhance mass transfer. However, we can draw general conclusions from Fig. 7b to d.

When the goal of using enzyme microreactor is converting the substrate to products, diffusion limitation is not desirable, as it reduces volumetric productivity (conversion per volume). When the residence time is much higher than the critical time given in this article, the reduction in the efficiency is very small. In contrast, when the residence time is lower than the critical time, the reduction in reactor efficiency is significant (>10%). Such a significant efficiency reduction is most likely to occur with wide microchannels (Fig. 7b), high enzyme concentrations (Fig. 7c), and low substrate concentrations (Fig. 7d).

5. Conclusions

The hydrolysis of *ortho*-nitrophenyl-β-D-galactopyranoside catalyzed by β-galactosidase from *K. lactis* was shown to follow Michaelis–Menten kinetics on bench scale and microscale. The kinetic parameters on both scales were the same. With the time scales applied during the experiments, the reaction seemed to be unaffected by diffusion limitation. Diffusion limitation was observed with experimental residence times below a few seconds. At these short residence times, the volumetric efficiency of the enzyme microreactor (conversion per volume) decreased. The critical residence time, where diffusion significantly limits the conversion, increased quadratically with channel width, increased with enzyme concentration, and decreased with substrate concentration. Estimations based on numerical calculations rather than the Da_{II} number can be used in wider range of conditions; it can be used in non-ideal situations. An enzyme microreactor can be run most efficiently when these factors receive appropriate attention.

Acknowledgements

The research described in this article was co-financed by the EU Program INTERREG IIIA of The Euregion Rijn-Waal and by the ministries of Economic Affairs of the Netherlands and Nordrhein-Westfalen.

References

[1] C.B. Cohen, E. Chin-Dixon, S. Jeong, T.T. Nikiforov, A microchip-based enzyme assay for protein kinase A, Anal. Biochem. 273 (1999) 89–97.
[2] A.G. Hadd, D.E. Raymond, J.W. Halliwell, S.C. Jacobson, J.M. Ramsey, Microchip device for performing enzyme assays, Anal. Chem. 69 (1997) 3407–3412.
[3] M. Lee, A. Srinivasan, B. Ku, J.S. Dordick, Multienzyme catalysis in microfluidic biochips, Biotechnol. Bioeng. 83 (2003) 20–28.
[4] W.D. Ristenpart, J. Wan, H.A. Stone, Enzymatic reactions in microfluidic devices: Michealis–Menten kinetics, Anal. Chem. 80 (2008) 3270–3276.
[5] A. Srinivasan, X. Wu, M. Lee, J.S. Dordick, Microfluidic peroxidase biochip for polyphenol synthesis, Biotechnol. Bioeng. 81 (2002) 563–569.
[6] J.W. Swarts, P. Vossenberg, M.H. Meerman, A.E.M. Janssen, R.M. Boom, Comparison of two-phase lipase catalyzed esterification on micro and bench scale, Biotechnol. Bioeng. 99 (2008) 855–861.
[7] H. Song, R.F. Ismagilov, Millisecond kinetics on a microfluidic chip using nanoliters of reagents, J. Am. Chem. Soc. 125 (2003) 14613–14619.
[8] B. Zheng, R.F. Ismagilov, A microfluidic approach for screening submicroliter volumes against multiple reagents by using preformed arrays of nanoliter plugs in a three-phase liquid/liquid/gas flow, Angew. Chem. Int. Edit. 44 (2005) 2520–2523.
[9] H.F. Arata, Y. Rondelez, H. Noji, H. Fujita, Temperature alteration by an on-chip microheater to reveal enzymatic activity of β-galactosidase at high temperatures, Anal. Chem. 77 (2005) 4810–4814.
[10] H. Mao, T. Yang, P.S. Cremer, A microfluidic device with a linear temperature gradient for parallel and combinatorial measurement, J. Am. Chem. Soc. 124 (2002) 4432–4435.
[11] H. Mao, T. Yang, P.S. Cremer, Design and characterization of immobilized enzymes in microfluidic systems, Anal. Chem. 74 (2002) 379–385.
[12] J. Wang, M.P. Chatrathi, B. Tian, Microseparation chips for performing multienzymatic dehydrogenase/oxicase assays: Simultaneous electrochemical measurement of ethanol and glucose, Anal. Chem. 73 (2001) 1296–1300.
[13] A.K. Sharp, G. Kay, M.D. Lilly, The kinetics of beta-galactosidase attached to porous cellulose sheets, Biotechnol. Bioeng. 11 (1969) 363–380.
[14] W.E. Hornby, M.D. Lilly, E.M. Crook, Some changes in the reactivity of enzymes resulting from their chemical attachment to water-insoluble derivatives of cellulose, Biochem. J. 107 (1968) 669–674.
[15] M.D. Lilly, W.E. Hornby, The kinetics of carboxymethylcellulose–ficin in packed beds, J. Biochem. 100 (1966) 718–723.
[16] K. Kanno, H. Maeda, S. Izumo, M. Ikuno, K. Takeshita, A. Tashiro, M. Fuji, Rapid enzymatic transglycosylation and oligosaccharide synthesis in a microchip, Lab. Chip. 2 (2002) 15–18.
[17] T. Maruyama, J. Uchida, T. Ohkawa, T. Futami, K. Katayama, K. Nischizawa, K. Sotowa, F. Kutoba, N. Kamiya, M. Goto, Enzymatic degradation of *p*-cholorophenol in a two-phase flow microchannel system, Lab. Chip. 3 (2003) 308–312.
[18] N. Kockmann, M. Engler, P. Woias, Theoretische und experimentelle Untersuchungen der Mischvorgänge in T-förmigen Mikroreaktoren - Teil 3: Konvektives Mischen und chemische Reaktionen, Chem-Ing-Tech. 76 (2004) 1777–1783.
[19] C.R. Wilke, P. Chang, Correlation of diffusion coefficients in dilute solutions, AIChE J. 1 (1955) 264–270.
[20] D. Cavaille, D. Combes, Characterization of beta-galactosidase from *Kluyveromyces lactis*, Biotechnol. Appl. Biochem. 22 (1995) 55–64.
[21] R. Dickson, L.R. Dickson, J.S. Markin, Purification and properties of an inducible β-galactosidase isolated from the yeast *Kluyveromyces lactis*, J. Bacteriol. 137 (1979) 51–61.